# Structural Investigation of Micelles Formed by an Amphiphilic PEP−PEO Block Copolymer in Water

**Andreas Poppe, Lutz Willner,* Jürgen Allgaier, Jörg Stellbrink, and Dieter Richter**

*Institut für Festkörperforschung, Forschungszentrum Jülich GmbH, D-52425 Jülich, Germany*

*Received April 7, 1997; Revised Manuscript Received September 16, 1997*[⊗]

ABSTRACT: Micelles of a poly(ethylene-*co*-propylene)-*block*-Poly(ethylene oxide) (PEP−PEO) copolymer in water were investigated by small angle neutron scattering (SANS), dynamic light scattering (DLS), and viscometry. The block copolymer was built of a partially deuterated PEP block and a hydrogeneous PEO block with an overall molecular weight of $11.1 \times 10^3$. The SANS measurements were performed at four contrasts in order to get detailed structural information about the micellar aggregates. The different scattering curves could be described very well by a spherical core−shell model with constant density in both parts. The sharp edges of the polymer density distribution were smeared by multiplication with a Gaussian in *Q*-space. The model yielded a core radius of $R_C = 176$ Å and an overall micellar radius of $R_M = 294$ Å. The smearing ranges were 11 and 32 Å, respectively. The fit further yielded an aggregation number of $P = 2430$. DLS measurements reveal a narrow monomodal distribution of relaxation frequencies, indicating the existence of only one aggregated species. The obtained hydrodynamic radius, $R_H = 339$ Å, as well as the radius determined by viscosity measurements, $R_V = 324$ Å, are consistent with the result of the model fitting. The unusually large aggregation number could be explained by the large interfacial tension between water and PEP in terms of simple thermodynamic models.

## 1. Introduction

During the past years, the micellization properties of amphiphilic block copolymers in water have attracted the attention of many research groups. In particular, polystyrene-*block*-poly(ethylene oxide) (PS−PEO) systems have been investigated intensively.[1−7] Recently, the synthesis of well-defined polyalkane−poly(ethylene oxide) block copolymers with either polyethylene (PE), poly(ethylene-*co*-propylene) (PEP), or poly(ethylethylene) (PEE) as the alkane block has been reported.[8−10] These new polymers show the same chemical design as the well-known low molecular weight alkane−oxyethylene ($C_n(EO)_m$) surfactants. The bulk-phase behavior of PEE−PEO block copolymers of relatively low molecular weights was found to resemble the behavior of both high molecular weight block copolymers and low molecular weight nonionic surfactant solutions.[11]

In dilute aqueous solution these amphiphilic block copolymers self-assemble into micelles with the polyalkane as the insoluble core and PEO as the soluble shell. From the extreme incompatibility of the polyalkane with PEO and water a sharp core/shell interface is expected. If the insoluble block is made of a low $T_g$ material like PEP, the dissolution of the polymer is assumed to yield aggregates which are in thermodynamical equilibrium at room temperature. In contrast, high-$T_g$ materials like PS as the micellar core can lead to structures being not in thermodynamic equilibrium due to the frozen state of the material. The expected sharp interface as well as the thermodynamic equilibrium facilitate a quantitative interpretation on the basis of current micellar models.[12−14] Thus, the PEP−PEO/water system can be regarded as a model system for studying fundamental properties of micelle formation.

The general aim of our work is to explore the aggregation behavior of the PEP−PEO system in water at low polymer concentrations. As a starting point for a systematic investigation, we describe here the structural examination of micelles formed by a PEP−PEO block copolymer in aqueous solution. The block copolymer is composed of a partially deuterated PEP block and a hydrogenous PEO block having a weight fraction of 46% PEP and an overall molecular weight of $11.1 \times 10^3$. The characterization of the micelles was performed by SANS, DLS, and viscometry. It has been demonstrated that SANS in combination with contrast variation is a powerful method to investigate micellar systems[15−18] and it was also shown that the structure of the micelles can be quantitatively evaluated by model fitting to the experimental data.[16−18]

## 2. Experimental Section

**2.1. Synthesis and Characterization of the PEP−PEO Block Copolymer.** The PEP−PEO block copolymer was synthezised by anionic polymerization. All manipulations were performed under high vacuum in glass reactors provided with break seals for the addition of reagents. The preparation of the initiators and the purification procedures for monomers and solvents to the standards required for anionic polymerization have been described elsewhere.[9]

The anionic polymerization of the block copolymer was realized in a two-step process, because the synthesis of the two blocks requires different reaction conditions. Polyisoprene with a high degree of 1,4-microstructure, the parent component of PEP, demands organolithium initiators and hydrocarbon solvents, whereas the polymerization of EO is performed in polar solvents using sodium or potassium initiators.

In the first step, fully deuterated isoprene was polymerized in benzene with *sec*-butyllithium as initiator. The end capping with ethylene oxide (EO) yielded d-polyisoprene functionalized with a hydroxyl end group (PI−OH). The polymer was hydrogenated with $H_2$ to the corresponding PEP−OH using a conventional $Pd/BaSO_4$ catalyst.

In the second polymerization step, cumylpotassium was used to transfer PEP−OH into the macroinitator PEP−OK. Therefore, PEP−OH was dissolved in dry THF and titrated with a solution of the deep red cumylpotassium in THF. The titration was stopped after a slight orange color in the polymer solution persisted for 5 min, indicating the complete deprotonation of the polymeric OH groups. The PEP−PEO block

* To whom correspondence should be addressed.

[⊗] Abstract published in *Advance ACS Abstracts,* November 1, 1997.

S0024-9297(97)00470-1 CCC: $14.00 

**Table 1. Molecular Weight Characterization of the PEP−PEO Block Copolymer**

| | $M_n$ | $M_w/M_n$ | wt % PEP | wt % PEO |
|---|---|---|---|---|
| PEP−OH | 5 130[a] | 1.02[c] | | |
| PEP−PEO | 11 100[b] | 1.03[c] | 46[b] | 54[b] |

[a] VPO. [b] Calculated from $M_n$ (VPO) of PEP−OH and the composition obtained by NMR. [c] SEC.

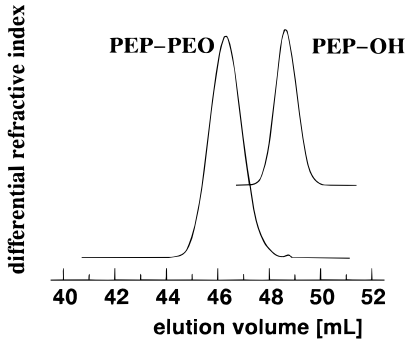


**Figure 1.** SEC traces of the PEP−OH precursor and the block copolymer PEP−PEO.

copolymer was obtained after polymerizing the calculated amount of hydrogenous EO in THF at 50 °C for 3 days. The reaction was terminated with acetic acid and the product precipitated twice in acetone at −10 to −20 °C. A more detailed description of the polymer synthesis is given elsewhere.[9]

Size exclusion chromatography (SEC) experiments were carried out at 30 °C, using a Waters 150C instrument. Four $\mu$-Styragel columns with a porosity range from $10^5$ to 500 Å and one ultra-Styragel column of continuous porosity were used together with a differential refractometer. The eluant was a mixture of THF and *N*,*N*-dimethylacetamide (90:10 by volume). In all experiments the flow rate was 1 mL/min. PS standards (Tosoh Corp.) were used for the calibration. The number average molecular weight ($M_n$) of the PEP−OH was measured with a Knauer vapor pressure osmometer at 45 °C. The solvent was benzene, which was distilled from $CaH_2$. The $M_n$ values were obtained using a calibration function of the type $(\Delta V/c)_{c\to 0} = KM_n^{\alpha}$, where $\Delta V$ is the change in voltage of the thermistors and $c$ is the concentration.[19] The calibration constants $K$ and $\alpha$ were obtained using benzile and PS standards of $440 \le M_n \le 9600$.

The copolymer composition was determined by $^{13}$C-NMR spectroscopy in $CDCl_3$ using a 500 MHz Bruker spectrometer.

Table 1 shows the molecular weight characterization of the PEP−OH precursor and the PEP−PEO block copolymer. The $M_n$ value of the PEP−OH obtained by vapor pressure osmometry (VPO) agrees very well with the result obtained from titration of PEP−OH with cumylpotassium ($M_n$ (titr) = 5180). With the amount of polymer and the concentration of the cumylpotassium solution, the titration can be considered as end group analysis for the determination of $M_n$. The narrow molecular weight distributions $M_w/M_n$ and the absence of homopolymer in the block copolymer, found by SEC (Figure 1), reveal together with the VPO and titration results the high quality of the material.

The completeness of the hydrogenation reaction yielding PEP−OH, and the deuterium and hydrogen contents of the PEP block were analyzed by $^1$H-NMR spectroscopy. The disappearance of the resonances associated with the olefin protons after hydrogenation revealed complete saturation of the double bonds. The D/H ratio was determined by examination of known amounts of PEP−OH together with the reference 1,1,2,2-tetrabromoethane. Comparing the polymer and reference signal intensities, we found a value of $C_5D_{6.37}H_{3.63}$ per monomer unit. This result indicates that during the hydrogenation reaction not only double bonds are saturated but also a considerable exchange of D by H occurs.

**2.2. Characterization of Micelles. Small Angle Neutron Scattering.** Neglecting interparticle scattering contributions, the coherent macroscopic scattering cross section of a SANS experiment $(d\Sigma/d\Omega)(Q)$ is of the general form

$$\frac{d\Sigma}{d\Omega}(Q) = \frac{N_z}{V}\langle|A(Q)|^2\rangle \tag{1}$$

where $N_z$ denotes the number of scatterers, $V$ is a reference volume, and $A(Q)$ is the intraparticle scattering amplitude. The scattering vector $Q$ is given by $4\pi \sin(\theta/2)/\lambda$, where $\theta$ is the scattering angle and $\lambda$ is the neutron wavelength.

For a particle consisting of a core−shell structure, the scattering amplitude, $A_{C,Sh}(Q)$, can be written as follows:

$$A_{C,Sh}(Q) = V_M(\rho_{Sh} - \rho_S)A_M(Q) + V_C(\rho_C - \rho_{Sh})A_C(Q) \tag{2}$$

with $\rho_C$, $\rho_{Sh}$, and $\rho_S$ as the scattering length densities of the core (C), the shell (Sh), and the solvent (S). The scattering length densities of the individual components $i$ involved are calculated by

$$\rho_i = \frac{\sum b_z}{v_i} \tag{3}$$

where $b_z$ is the coherent scattering length of an individual atom z in the solvent molecule or in the repeat unit of the polymer, $v_i$ are the respective volumes. $V_M$ and $V_C$ denote the volume of the overall micelle and the core; $A_M(Q)$ and $A_C(Q)$, the corresponding scattering amplitudes. Equation 2 reduces to simple forms, if the condition $\rho_{Sh} = \rho_S$ or $\rho_C = \rho_S$ is fullfilled. Concerning the first case, one obtains for the intraparticle scattering amplitude:

$$A_{C,Sh}(Q) = V_C(\rho_C - \rho_{Sh})A_C(Q) \tag{4}$$

This scenario is denoted as core contrast. For the second case, the shell contrast, eq 2 simplifies to

$$A_{C,Sh}(Q) = (\rho_C - \rho_{Sh})(A_C(Q)V_C - A_M(Q)V_M) \tag{5}$$

The SANS experiments were performed on the KWSI instrument at the research reactor FRJ2 at the Forschungszentrum Jülich GmbH. The block coplymer micelles were studied under core and shell contrast and, additionally, under an intermediate contrast and in pure $D_2O$. For the PEP chains in the core of the micelle, a scattering length density of $\rho_{PEP} = 4.577 \times 10^{10}$ cm$^{-2}$ was calculated. The calculation was performed using eq 3 on the basis of the H/D composition obtained from the NMR measurement. The scattering length density of PEO, $\rho_{PEO}$, was calculated to be $0.6376 \times 10^{10}$ cm$^{-2}$. The volume of a repeat unit was calculated with the density, $d = 1.125$ g/cm$^3$, of amorphous PEO. In order to obtain matching conditions, mixtures of $D_2O/H_2O$ were prepared according to the simple additivity rule:

$$\rho_S = \phi_{D_2O}\rho_{D_2O} + (1 - \phi_{D_2O})\rho_{H_2O} \tag{6}$$

with $\phi_{D_2O}$ as the volume fraction of $D_2O$ in the isotopic water mixture. $\rho_{D_2O} = 6.404 \times 10^{10}$ cm$^{-2}$ and $\rho_{H_2O} = -0.562 \times 10^{10}$ cm$^{-2}$ denote the scattering length densities of the pure solvents. Thus, core contrast, $\rho_S = \rho_{PEO} = \rho_{Sh}$, is obtained with $\phi_{D_2O} = 0.171$ and shell contrast, $\rho_S = \rho_{PEP} = \rho_C$, with $\phi_{D_2O} = 0.734$. For the intermediate contrast, a volume fraction of $\phi_{D_2O} = 0.449$ was taken, leading to a $\rho_S$ of $2.607 \times 10^{10}$ cm$^{-2}$.

Using these $H_2O/D_2O$ mixtures and pure $D_2O$ block copolymer solutions with a polymer volume fraction of $\phi = 1\%$ were prepared. In order to facilitate the solubilization process, the water/block copolymer mixtures were heated to 50 °C for 2 h. The resulting solutions were slightly turbid. The samples were studied in 2 mm quartz cells, except for the solution with the highest $H_2O$ content, which was measured in a cell with 1 mm path length in order to avoid low transmission due to incoherent scattering. The transmissions of these samples were between 0.37 and 0.57. In order to determine the solvent

background, all isotopic water mixtures were measured separately under the same conditions. The SANS experiments were carried out at sample to detector distances of $L = 4$, 8 and 20 m, covering a $Q$-range of 0.003 Å$^{-1} \leq Q \leq$ 0.08 Å$^{-1}$. The collimation was positioned at the same length as the corresponding sample to detector distance. The raw data were corrected for electronic background and the scattering of the empty cell was subtracted. The data were corrected for different detector cell efficiency and calibrated to absolute units by a Lupolen secondary standard[20] according to

$$\frac{d\Sigma}{d\Omega}(Q)=\frac{L^S h^S T^S \mathrm{MON}^S I(Q)}{LhT\mathrm{MON}I^S(0)}\left(\frac{d\Sigma(0)}{d\Omega}\right)^S \quad (7)$$

Here S refers to the standard. MON denotes the total amount of monitor counts, $h$ the sample thickness, $L$ the sample to detector distance, and $T$ the transmission. $I(Q)$ is the scattered intensity, and $I^S$ (0), the measured intensity of the standard at $Q = 0$. The value of $(d\Sigma(0)/d\Omega)^S$ for the Lupolen standard has been calibrated with vanadium to be 1.781 55 cm$^{-1}$. Finally, the scattering contribution of the solvent and the calculated incoherent scattering of the protonated portion of the polymer was subtracted.

**Dynamic Light Scattering.** In order to get a maximum degree of comparability of the experiments, all solutions used for dynamic light scattering (DLS)[21,22] were prepared by dilution of a stock solution of 1% volume fraction in $D_2O$ already used for the SANS experiments. After dilution, each solution was heated for about 2 h at 50 °C, in order to ensure the thermodynamic equilibrium. Four samples were prepared, covering a concentration regime between $\phi = 0.1\%$ and $\phi =$ 1%. The solutions were filtered through 0.2 $\mu$m Anotop filters (Whatman) into the thoroughly cleaned sample cells (Hellma). The refractive index ($n_d = 1.328$) and density of the solvent ($d$ = 1.11 g/cm$^3$) were taken from the literature,[23] the absolute viscosity was determined to be $\eta_0 = 1.251$ cP.

DLS experiments were performed on a ALV SP-125 (ALV) compact goniometer in a homodyne setup using an argon ion laser (Coherent, Innova 90-4), operating with vertically polarized light at $\lambda_0 = 514.5$ nm, $I_0 = 50-800$ mW TEM$_{00}$. Intensity autocorrelation functions $g_2(Q, t)$ were recorded with an ALV 5000 E (fast version, 319 channels) multi-$\tau$ digital correlator covering a time window from 12.5 ns up to several hours. The scattering vector $Q$ for light scattering is given by $4\pi n_d \sin(\Theta/2)/\lambda_0$, with $\lambda_0$ the wavelength in vacuum. The experimental coherence factor $f_c$ was determined by use of PS−latex spheres (PSS) to be $f_c = 0.92$. Due to the use of a dual detector system (ALV-SO/SIPD) operating in "pseudo"-cross correlation mode, even the first channels could be recorded without any distortion from electronic noise. All measurements were performed at 20.0 ± 0.1 °C in the angular range $28° \leq \Theta \leq 120°$, yielding a $Q$-range from $7.84 \times 10^{-4}$ to $2.8 \times 10^{-3}$ Å$^{-1}$.

The obtained intermediate scattering functions $f_c g_1(Q, t) = \sqrt{g_2(Q,t) - 1}$ were analyzed independently by (i) the cumulant method,[24] which expands $\ln(f_c g_1(Q, t))$ in a power series of $t$: $\ln(f_c g_1(Q, t)) = \mu_0 - \mu_1 t + (1/2!)\mu_2 t^2 - \ldots$, with a first cumulant $\mu = \bar{\Gamma}$, the mean relaxation frequency, and a reduced second cumulant $\mu_2/\bar{\Gamma}^2$ related to the polydispersity of the sample, and (ii) the inverse Laplace transformation using the regularization algorithm of the CONTIN program.[25,26] To account for particle interactions in dilute solution, a virial expansion can be made, which describes the concentration dependence of the mutual diffusion coefficient $D_m(\phi) = \bar{\Gamma}(\phi)/Q^2$.

$$D_m(\phi) = D_0(1 + k_D^{\phi}\phi) \quad (8)$$

After extrapolation to infinite dilution, the hydrodynamic radius of the scattering particles can be derived from the Stokes−Einstein relation:

$$R_H = \frac{k_B T}{6\pi\eta_0 D_0} \quad (9)$$

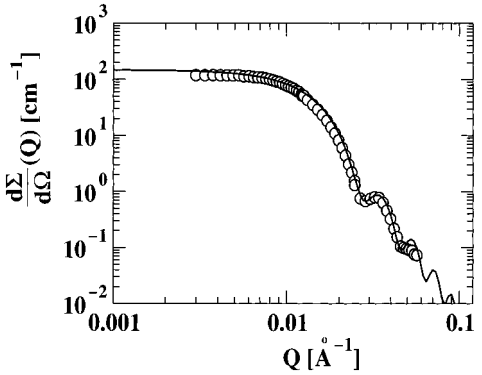


**Figure 2.** Absolute SANS data under core contrast. The solid line represents the result of the model fit performed on an absolute intensity scale.

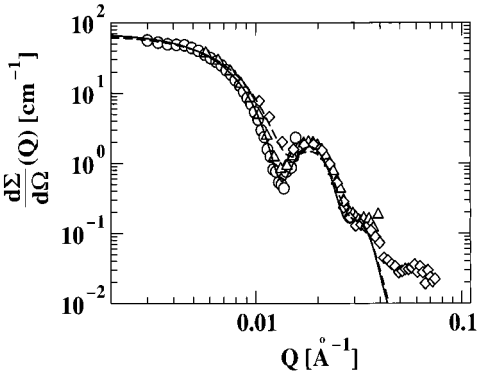


**Figure 3.** Absolute SANS data under shell contrast. The solid line represents the result of the model fit convoluted with the instrumental resolution at 20 m detector distance; the dashed line, the one convoluted with the instrumental resolution at 4 m detector distance. The cross section was a variable during the fitting procedure.

with $k_B$, $T$, and $\eta_0$ the Boltzmann constant, the absolute temperature, and the solvent viscosity, respectively.

**Viscometry.** An Ostwald microviscometer and an automated measuring system of Schott-Geräte, Mainz, Germany, was used to determine the specific viscosities $\eta_{sp}$ of six PEP−PEO block copolymer solutions in the concentration range between $c = 0.001$ and 0.01 g/mL at 20 °C. With the used type of viscometer, the flow times were in the range where no Hagenbach corrections had to be performed. The intrinsic viscosity of the system, $[\eta] = 7.928$ mL/g, was determined from a Huggins plot ($\eta_{sp}/c$ versus $c$) in the limit $c \rightarrow 0$.

## 3. Results

**SANS Measurements.** The coherent macroscopic scattering cross sections $(d\Sigma/d\Omega)$ $(Q)$ for each contrast, evaluated according to the procedure described in the Experimental Section, are shown in Figures 2−5. In all cases, strong scattering is observed, indicating the formation of large aggregates. The curves exhibit a well-pronounced secondary maximum and even a weak third maximum at higher $Q$-values, displaying the existence of aggregates with well-defined structure. Especially, the sharpness of the minima in the core (Figure 2) and shell (Figure 3) contrast reveals a narrow size distribution, a sharp core/shell interface, and a sharp density cutoff at the periphery of the micelle. The scattering curve obtained at the intermediate contrast (Figure 4) decreases in intensity at low $Q$. In this case, the scattering length density of the respective isotopic water mixture is not far from the average scattering length density of the block copolymer. Under the condition of a zero average contrast, the intensity at $Q$

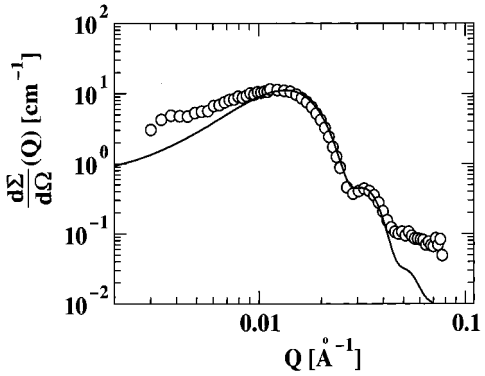


**Figure 4.** Absolute SANS data under intermediate contrast. The solid line represents the result of the model fitted with variable cross section.

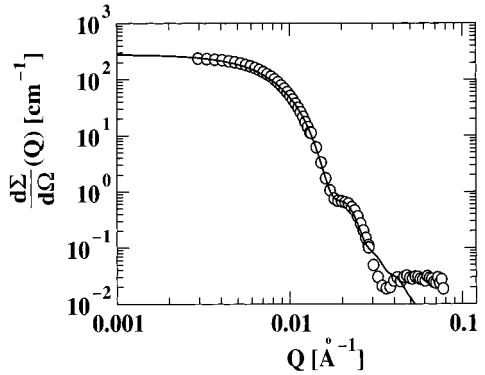


**Figure 5.** Absolute SANS data under $D_2O$ contrast. The solid line represents the result of the model fitted with variable cross section.

= 0 would be zero. In pure $D_2O$ (Figure 5) the maximum contrast condition is obtained, leading to the highest forward scattering of all measurements.

In order to analyze the structure of the micelle, model fitting was performed to the experimental data. As a model, a spherical core/shell structure was used. Thereby, the scattering length density distribution was assumed to be homogeneous over the core and the shell, respectively. The density cutoff at the PEP/PEO−water interface and the outer periphery of the micelle was smeared by multiplication with a Gaussian in $Q$-space. The scattering amplitudes introduced in eq 2 for this model are given by

$$A_{M,C}(Q) = \frac{3(\sin(QR_{M,C}) - QR_{M,C}\cos(QR_{M,C}))}{(QR_{M,C})^3}\exp\left(-\frac{\sigma_{M,C}{}^2Q^2}{4}\right) \quad (10)$$

where the indices C and M refer either to the core or to the micelle. The effect of smearing is given in terms of the parameters $\sigma_{M,C}$.

Since the corona is swollen with water the actual scattering length density $\rho_{Sh}$ of this part differs from that of pure PEO. A homogeneous density distribution is assumed in the model and, therefore, an average scattering length density of the shell can be defined

$$\rho_{Sh} = \phi_{S,Sh}\rho_S + (1 - \phi_{S,Sh})\rho_{PEO} \quad (11)$$

where $\rho_S$ is the scattering length density of the isotopic water mixture. $\phi_{S,Sh}$ denotes the volume fraction of water in the corona, which consistently is calculated by

$$\phi_{S,Sh} = 1 - \frac{Pv_{PEO}N_{PEO}}{(4/3)\pi R_M{}^3 - (4/3)\pi R_C{}^3} \quad (12)$$

where $v_{PEO}$ represents the volume of a PEO repeat unit. $P$ is the aggregation number of the micelles given by

$$P = \frac{V_C}{v_{PEP}N_{PEP}} \quad (13)$$

where $V_C$ denotes the volume of the core, given by $(4/3)\pi R_C{}^3$, $v_{PEP}$ the volume of a PEP repeat unit and $N_{PEP}$ the degree of polymerization of the PEP part in the block copolymer.

The number density of scatterers $N_z/V$ was calculated by the following expression:

$$\frac{N_z}{V} = \frac{\phi}{V_{PEP-PEO}P}N_A \quad (14)$$

$\phi$ denotes the volume fraction of block copolymer in solution, $V_{PEP-PEO}$ is the molecular volume of PEP−PEO, and $N_A$ is the Avogadro number.

The model based on eqs 1, 2, and 10−14 was applied to describe the experimental scattering data. Five parameters of the model $P$, $R_M$, $\sigma_M$, $\sigma_C$, and $\phi_{S,Sh}$ are independent variables (Table 2). For the calculation, a standard fitting routine was used, which additionally allowed the computation of the different contrasts simultaneously. In order to obtain a good coincidence with the experimental data, the theoretical curves were convoluted with a Gaussian type resolution function according to Pedersen et al.[27] taking into account the wavelength spread and collimation of the SANS machine.

In the first step of the evaluation, the scattering curve of the core contrast was fitted independently using the condition defined in eq 4. The scattering length density of the $H_2O/D_2O$ mixture, $\rho_S = 0.6376 \times 10^{-10}$ cm$^{-2}$, as well as the scattering length density of the core, $\rho_{PEP} = 4.577 \times 10^{-10}$ cm$^{-2}$, were introduced as fixed parameters. For $N_{PEO}$ and $N_{PEP}$ we took the values obtained from the combination of different characterization techniques. The aggregation number, $P$, and the smearing of the core−shell interface, $\sigma_C$, were the adjustable parameters in the fitting procedure. Figure 2 presents the resulting fit. We note that, on an absolute scale, perfect agreement between the data and the theoretical form factor of a sphere is achieved. For the aggregation number we find $P = 2430$, a very large number considering the small molecular weight of the involved polymers. The aggregation number translates into a core radius of $R_C = 176$ Å with a very small smearing of $\sigma_C = 11$ Å or 6.2%, which may be due to a small polydispersity or/and due to some surface roughness.

In a second step all scattering data at different contrasts were fitted simultaneously. Thereby, the parameters obtained in the first step were kept fixed, while the outer micellar radius, $R_M$, and the smearing of the outer edge, $\sigma_M$, were the variables. As it turned out, with this approach the data could not be fitted on an absolute intensity scale. The experimentally observed macroscopic cross sections, $d\Sigma/d\Omega$, were found to be systematically below the expected values, indicating problems with normalization or the actual contrast.

In order to proceed further, we relaxed the condition of absolute normalization, which was successful in the case of the core contrast, and allowed the cross sections

to vary in the fit. Figures 3−5 display the results. For both the shell and the $D_2O$ contrast, very good agreement is achieved in the lower $Q$-range. This good description is achieved with a common set of structural parameters. For the outer micellar radius $R_M = 294$ Å, and a smearing of $\sigma_M = 32$ Å, is obtained. The micellar molecular weight is calculated to be $M = PM_n = 2.7 \times 10^7$.

The deviation at higher $Q$-values in all three cases originates from the blob structure of the polymer chains in the corona. For $Q \geq \xi^{-1}$, where $\xi$ is a typical blob size, the chain structure reveals itself and leads to extra scattering at high $Q$. Since these scattering contributions are not considered in the theoretical expression, the $Q$-range used for the fit was limited to $0.003\ \text{Å}^{-1} \leq Q \leq 0.021\ \text{Å}^{-1}$. The deviations do not appear for the curve of the core contrast, since the individual PEP chains are not contrasted by the solvent. We draw attention to Figure 3 displaying the scattering curves under shell contrast. They present the influence of the instrumental resolution for different detector positions, which was convoluted with the theoretical cross section. While for the 20 m detector distance the instrumental resolution is high and consequently the deep minimum of $d\Sigma/d\Omega$ at $Q \approx 0.01\ \text{Å}^{-1}$ is well reproduced, at 4 m detector distance the resolution is much broader and the minimum is much less pronounced both in the data and in the resolution-convoluted form factor.

For the intermediate contrast (Figure 4) the calculated cross section agrees well at intermediate $Q$-values but differs not only at high but also at low $Q$ from the data. The reduction of the forward scattering at intermediate $Q$-values depends sensitively on the proper choice of the solvent scattering length density, which needs to be at the average of both components. Obviously, this is not the case in our experiment.

We now turn to the absolute cross sections. Though the polymers are very well characterized and there is little doubt about molecular weight and composition of the diblocks, apparently the PEO chains do not scatter enough. This is most clearly evident for the data under shell contrast. Given the nearly identical scattering volume of the PEP and the PEO chains under core and shell scattering contrast, the same forward scattering should have been observed. Looking at Figures 2 and 3, we realize a factor of 2 difference in the observed intensities. This qualitative observation manifests itself also in the deviations between the observed cross sections and those obtained from the fit. Under shell and $D_2O$ contrast, a factor of 2.0 is missing, while under intermediate contrast the deviation is 1.16.

In order to exclude experimental errors the SANS measurements in core and shell contrast were repeated under the same conditions on the D11 instrument at the high-flux reactor in Grenoble, France. The results obtained were within experimental error identical to those before. Moreover, NMR and SEC measurements after the SANS experiments reveal that no chain degradation or isotope exchange has occurred during the experiments. We are thus confronted with the observation that the experimentally determined scattering length density of PEO chains is significantly lower than what is calculated on the basis of eq 3. A similar discrepancy between nominal molecular weight and SANS molecular weight was observed by Vennemann et al.[28] on the PEO homopolymer but was not discussed further.

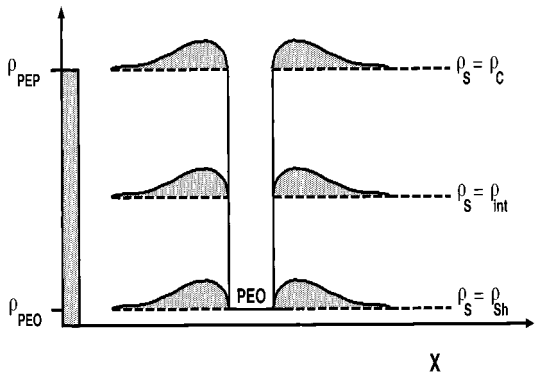


**Figure 6.** Scattering length densities plotted versus the spatial coordinate of the PEP−PEO system. The rectangular gap in the middle of the graph represents the PEO block. The dashed lines indicate the average solvent scattering length densities, $\rho_S$, for core, shell, and intermediate contrast. At the origin the scattering length density of the core, $\rho_{PEP}$ is shown as a column. E.g., for $\rho_S = \rho_{PEO} = \rho_{Sh}$ the PEO chains are matched and we observe the PEP core. The dotted regions in the neighborhood of the PEO chain correspond to the density enhancement of the solvent mixture. The fit procedure provides only the integral of these regions, not their expansion or the maximum value of solvent compression separately. Since the absolute scattering length density of PEO is very small, the density enhancement for $\rho_S = \rho_{Sh}$ influences the scattering only a little, in particular in view of the large contrast between the core, $\rho_{PEP}$, and $\rho_{Sh}$. In the case of $D_2O$-rich solvent mixtures, e.g., shell contrast, the actual scattering of the micelles deviates from the expected by far. This is due to the high scattering contrast between the PEO and the solvent, where at the same time the core stays matched. The scattering of the intermediate contrast, $\rho_S = \rho_{int}$ is accordingly influenced in an intermediate way.

Given the correctness of the polymer characterization, which was cross checked in multiple ways, and the reproducibility of the neutron scattering data obtained from KWS1 in Juelich and D11 in Grenoble, we are forced to assume that the scattering density of PEO is modified by the water shell around the chain backbone, which would have to have a higher density than normal water.

Such a higher density shell of bound hydration water could qualitatively explain the observed trends. The protonated PEO block has a low scattering length density, $\rho_{PEO}$, similar to that of $H_2O$, while the deuterated PEP chain and $D_2O$ possess highly positive scattering length densities. Under core contrast the solvent is $H_2O$-rich with a small $\rho_S$ equal to $\rho_{PEO}$. Compared to the large contrast to the core, $(\rho_C - \rho_{PEO})^2$, a density enhancement of the solvent around the PEO chain would have a little effect on the observed absolute cross section (Figure 6). The picture changes under shell contrast. Then the core is matched out and a density enhancement of the $D_2O$-rich solvent around the chain would effectively screen the low scattering length density profile of the PEO chain and reduce the absolute cross section (Figure 6).

Quantitatively, we may formulate the scattering cross section of a PEO chain with the volume $N_{PEO}v_{PEO}$ surrounded by a water shell occupying a volume $\bar{\alpha}v_{PEO}N_{PEO}$ following eqs 1−3:

$$\frac{d\Sigma}{d\Omega}(Q\rightarrow 0) = \frac{N_Z}{V}\left[\frac{v_{PEO}\rho_{PEO} + \bar{\alpha}v_{PEO}(d_S^b/d_S)\rho_S}{v_{PEO} + \bar{\alpha}v_{PEO}} - \rho_S\right]^2 \times (N_{PEO}(v_{PEO} + \bar{\alpha}v_{PEO}))^2 \quad (15)$$

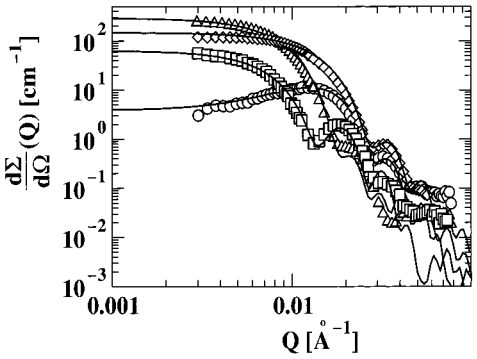


**Figure 7.** Scattering data and fit results obtained by the core/shell model in which the reduction of the PEO cross section due to hydration water is considered. The fit was performed on an absolute scale yielding a correction factor of $f = 0.25$.

where $N_{PEO}(v_{PEO} + \bar{\alpha}v_{PEO})$ is the volume occupied by the chain including the hydration shell. $d_S^b$ is the enhanced water density in the hydration shell. After some manipulations eq 15 becomes

$$\frac{d\Sigma}{d\Omega}(Q\rightarrow 0) = \frac{N_Z}{V}(N_{PEO}v_{PEO})^2[\rho_{PEO} + \rho_S\bar{\alpha}((d_S^b/d_S) - 1) - \rho_S]^2 \quad (16)$$

The scattering contrast between the polymer and the solvent is reduced by the factor $\rho_S\bar{\alpha}[(d_S^b/d_S) - 1]$, which turns to zero if there is no density enhancement. We note that the product of the volume proportionality factor $\bar{\alpha}$ and the density enhancement $[(d_S^b/d_S) - 1]$ enters; no independent information on one of the two quantities is revealed. This would require diffraction experiments with a spatial resolution sensitive to the molecular distances within the hydration shell.

Replacing $\rho_{PEO}$ in eq 11 by $\rho_{PEO} + \rho_S f$ with $f = \bar{\alpha}((d_S^b/d_S) - 1]$, we have repeated the fitting procedure, now varying $f$ and requiring the proper normalization of the cross sections. Figure 7 presents the obtained result. With this approach very good agreement both with respect to the absolute intensities and with respect to the scattering profiles is obtained. We draw particular attention to the data at intermediate contrast, which are now described naturally; because the effective PEO contrast is reduced, the zero-average contrast condition is not fulfilled and the theoretical curve does not decay to zero for low $Q$ but follows the data. For the correction factor we find $f = 0.25$, which appears very large to us. We note that this value is mainly influenced by the scattering data from the $D_2O$-rich samples, while the $H_2O$-rich core contrast experiment is not sensitive to $f$. Thus we cannot address possible isotope effects that would be suggested by a comparison with density measurements on h-PEO in $H_2O$. There, a decrease of the PEO molar volume of only 6% compared to the bulk was reported.[28] Further scattering experiments on h-PEO and d-PEO in different aqueous environments are planned in order to scrutinize this problem in more detail.

**Dynamic Light Scattering.** Intensity autocorrelation functions (icfs) obtained at different scattering angles are shown in a log−log plot in Figure 8 for the lowest volume fraction, $\phi = 0.1\%$. All icfs are fully relaxed; neither a decrease of the coherence factor $f_c$ nor baseline contributions $\geq 10^{-3}$ can be detected. The experimental data reveal just one relaxation process at all $Q$-values, as shown by comparison to a single exponential decay, also plotted in Figure 8 for $\Theta = 90°$.

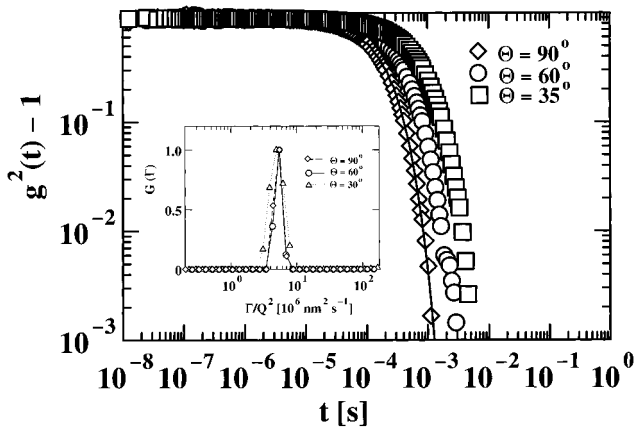


**Figure 8.** Intensity autocorrelation functions obtained at $\theta = 35$, 60, and 90° of the PEP−PEO block copolymer in water at $\phi = 0.1\%$ and $T = 20$ °C. The solid line is a fit to a single exponential decay. The insert displays the corresponding distribution of relaxation frequencies obtained by inverse Laplace transformation (CONTIN) plotted versus the reduced variable $\Gamma/Q^2$.

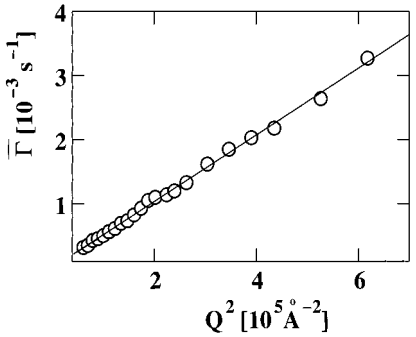


**Figure 9.** Relaxation frequency $\bar{\Gamma}$ plotted versus $Q^2$ for the sample of volume fraction 0.1%. The solid line represents the linear fit to the data.

Analysis of the initial decay of the icfs, i.e., applying the cumulant method, reveals a reduced second cumulant characteristic for a narrow size distribution of scatterers: $0.01 \leq \mu_2/\bar{\Gamma}^2 \leq 0.04$, slightly increasing with decreasing scattering angle. It has been shown,[29] that the reduced second cumulant can be related to the conventional polydispersity $M_w/M_n$ by

$$\mu_2/\bar{\Gamma}^2 = \nu^2(M_w/M_n - 1) \quad (17)$$

with $\nu$ the scaling exponent in the relation $D_0 \sim M^\nu$. Using $\nu = 0.56$ as found for PEO homopolymers,[30] a polydispersity of $1.03 \pm 0.02$ can be estimated from the high $Q$-data.

This narrow size distribution of the scattering particles is confirmed by the distribution of relaxation frequencies $G(\Gamma)$ obtained from inverse Laplace transformation (CONTIN[25,26]) shown in the inset of Figure 8. The results for $\bar{\Gamma}$ from cumulant expansion and inverse Laplace transformation differ by only 3% for this volume fraction. The diffusive character of the observed relaxation process is revealed by the inset of Figure 8 and Figure 9, where $\bar{\Gamma}$ is plotted versus $Q^2$. With increasing volume fraction, the solutions become slightly turbid; thus possible effects of multiple scattering have to be considered. At higher volume fractions, an additional small peak (≤3% amplitude) appears on the high-frequency side of the main peak in $G(\Gamma)$; see Figure

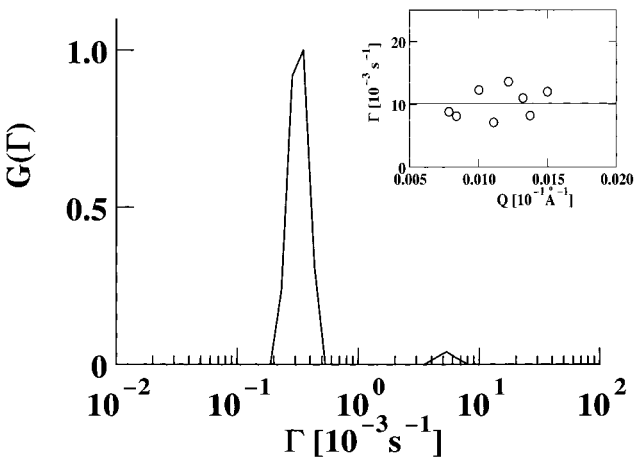


**Figure 10.** Dependence of the relaxation frequency Γ of the multiple scattering process on $Q$ of the $\phi = 0.5\%$ solution. The insert shows the $Q$-independence of the fast mode.

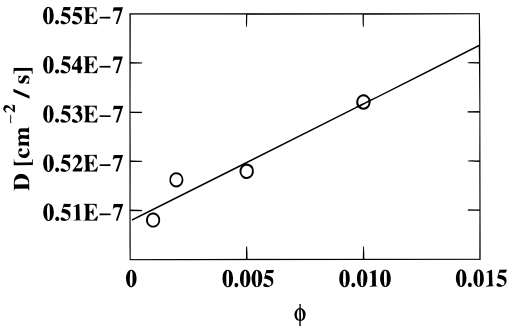


**Figure 11.** Dependence of the mutual translational diffusion coefficient on block copolymer volume fraction. The solid line represents the linear extrapolation to zero concentration.

**Table 2. Parameters of the Spherical Core/Shell Model**

| P | M | $R_M$/Å | $\sigma_M$/Å | $R_C$/Å | $\sigma_C$/Å | $\phi_{S,Sh}$ |
|---|---|---|---|---|---|---|
| 2430 | $2.7 \times 10^7$ | 294 | 32 | 176 | 11 | 0.744 |

**Table 3. Results of DLS and Viscometry**

| $D_0/10^{-8}$ cm$^{-2}$ s$^{-1}$ | $R_H$/Å | $k_D\phi$ | $R_V$/Å | $M_w/M_n$[a] |
|---|---|---|---|---|
| 5.06 | 339 | 4.7 | 324 | 1.03 |

[a] Estimated from the reduced second cumulant.

10. Parallel with the appearance of the fast mode, the reduced second cumulant increases to ≈0.2 and finally the experimental data can no longer be described by cumulant expansion. In the insert of Figure 10 the mean relaxation frequency of the fast mode as obtained from CONTIN is plotted versus scattering vector $Q$. Due to its $Q$ independence the fast mode was identified as multiple scattering contribution and separated according to Stepanek.[31] Because of its irrelevance for the problems under investigation it will not be discussed further. The mean relaxation frequency $\bar{\Gamma}$ derived from the main peak still shows the $Q^2$-dependence expected for translational diffusion at all volume fractions.

After extrapolation to infinite dilution, a hydrodynamic radius $R_H = 339$ Å of the micelles is derived from $D_0$ by use of the Stokes−Einstein relation (eq 9). The results of the dynamic light scattering experiments are summarized in Table 3 (Figure 11).

**Viscometry.** The viscometric radii of the micelles were calculated according to the following equation:

$$R_V = \left(\frac{3[\eta]M}{10N_A\pi}\right)^{1/3} \qquad (18)$$

where $[\eta] = 7.928$ mL/g is the intrinsic viscosity, $M = 2.7 \times 10^7$ is the molecular weight of the micelles as obtained from the model fitting of the SANS data, and $N_A$ is the Avogadro number. Thus, a viscometric radius of $R_V = 324$ Å was calculated. For a better comparison, this value is also listed in Table 3.

## 4. Discussion

**4.1. Micellar Parameters.** The aggregation behavior of a PEP−PEO block copolymer in water is examined by SANS, DLS, and viscometry. The results obtained by SANS and DLS reveal the existence of only one aggregated species. Large scale aggregates due to a secondary association as reported for the PS−PEO/water system[1] could not be observed. Association was also found for the PEO homopolymer in water[32] and attributed to the presence of an impurity.[33] The absence of large aggregates in the PEP−PEO/water system can therefore be taken as an additional indication for the purity of the block copolymer. The size of the aggregates does not change between $\phi = 1\%$ and $\phi = 0.1\%$, as can be seen from the linearity of the mutual diffusion coefficient $D_m$ in this concentration range. Moreover, it can be concluded that the critical micelle concentration is well below a polymer volume fraction of $\phi = 0.1\%$.

The evaluation of the SANS cross sections by model fitting shows that the observed aggregated species has a spherical core/shell geometry. The validity of this structure is underlined by the fact that an excellent agreement is obtained between theoretical and experimental curves by fitting simultaneously all measured contrasts with one set of parameters. The model parameters $P = 2430$, $R_M = 294$ Å, $R_C = 176$ Å, and $M = 2.7 \times 10^7$ indicate with respect to the low molecular weight of the block copolymer surprisingly large dimensions of the micelles. The large size of the aggregates is further established by the hydrodynamic radius, $R_H = 339$ Å, and by the viscometric radius, $R_V = 324$ Å. For hard spheres the static and the dynamic radii should be identical. The slightly larger values of $R_H$ and $R_V$ may be due to experimental uncertainty. It may also be explained by the fuzziness of the outer periphery of the micelle. Thus, by adding half of the smearing parameter to the micellar radius ($R_M + \sigma_M/2 = 310$ Å), a better agreement is obtained. Furthermore, the hydration of PEO can cause differences between hydrodynamic and static radii.

The good agreement of the core contrast measurement with the model curve reveals that the core consists of PEP only with a density equal to the bulk density of PEP. On the basis of the core/shell model it could be further concluded that the shell of the micelle is highly swollen with 74.4% water, although the absolute intensity could only be explained by assuming important hydration effects. From the smearing parameters $\sigma_{C,M}$ it is obvious that the core/shell interface as well as the density cutoff at the edge of the micelle is fairly sharp. It should be noted that the theoretical and experimental curves are in good agreement, assuming only small smearing effects for the core. Whether this smearing is due to polydispersity or due to genuine surface roughness cannot generally be decided on the basis of SANS experiments on spherical entities. Both have almost the same effect on the calculated scattering curves. The relatively large value of $\sigma_M$ must relate to the diffuse outer edge of the micelle rather than to polydispersity effects, which would have to be present also at the edge of the core. This assumption is

underlined by the DLS results, where a polydispersity of 1.03 was estimated from the reduced second cumulant.

The large dimensions of the micelle with respect to the relatively low molecular weights of the two blocks in the copolymer imply a strong stretching of the chains. The radius of gyration of the PEO homopolymer in the melt can be calculated by $R_G^2 = C_\infty M l_b^2/(6m_0)$, where $C_\infty = 5.7$ is the charateristic ratio of PEO, $l_b^2 = 2.1436$ Å$^2$ is the mean square bond length, and $m_0 = 14.6$ is the mean molecular weight per skeletal bond.[34] The use of this equation is justified by the fact that low molecular weight polymers in a good solvent have chain dimensions similar to those under $\theta$-conditions. By introducing the block molecular weight of $M_n$(PEO) = 5970, a radius of gyration of 29 Å is calculated. In order estimate the streching of the PEO chains in the shell of the micelle, a comparison with the end to end distance, which is given by $R_G\sqrt{6} = 71$ Å, has to be made. By use of a shell thickness of $R_M - R_C = 118$ Å, a stretching by a factor of ~1.7 can be calculated. This considerable elongation of the PEO chain in the shell of the micelle causes a high entropy loss, which has to be compensated for by a reduction in surface energy due to surface minimalization. The high value of the aggregation number of the micelle reflects this point. A more quantitative interpretation will be performed in the following section.

**4.2. Interpretation in Terms of Models for the Free Energy.** The free energy $F$ of a single chain incorporated in a micelle far away from the critical micellar concentration is approximated as a sum of three contributions:[12]

$$F = F_{int} + F_{Sh} + F_C \tag{19}$$

The first term $F_{int}$ denotes the interfacial contribution to the free energy associated with the core−corona interface, given by

$$F_{int} = \frac{4\pi R_C^2 \gamma}{P_{eq}} \tag{20}$$

where $\gamma$ denotes the surface tension and $P_{eq}$ the equilibrium aggregation number. The contributions $F_C$ and $F_{Sh}$ are related to chain stretching in the core and the shell, respectively. A modified type of the Alexander model[35] was used in order to estimate the contributions due to $F_{Sh}$. This model was originally developed to describe the free energy of a flat polymer brush, but it can be used as a first approximation for the free energy of the shell in micellar systems for the case of a small curvature of the core/shell interface. The free energy, $F_{Sh}$, in terms of the Alexander model comprises an elastic and an interaction part. The dominant part in this view is the interaction term and, therefore, the elastic contribution will be neglected. By application of this model to micellar aggregates, the shell is envisioned as a closed packed array of blobs of uniform size $\xi$, each assigned a free energy of $k_BT$. The free energy $F_{Sh}$ is then proportional to the number of blobs per chain:

$$F_{Sh} = k_B T n N_{Sh} l^{5/3} \xi^{-5/3} \tag{21}$$

where $k_B$ denotes the Boltzmann constant, $T$ the absolute temperature, and $n$ the number of skeletal bonds per repeat unit of the chain inside the shell. The length $l$ is defined by $l^2 = C_\infty l_b^2$, where $C_\infty$ denotes the characteristic ratio of the polymer and $l_b^2$ the mean square bond length. $N_{Sh}$ refers to the degree of polymerization, and $\xi$ is the blob size which is given by

$$\xi = \sqrt{\frac{4\pi R_C^2}{P_{eq}}} \tag{22}$$

In order to estimate the equilibrium aggregation number, minimization of $F$ with respect to $P_{eq}$ was performed on the basis of eqs 20−22. Thereby, the contribution $F_C$ due to the stretching of the core chains was neglected. By taking into account that

$$R_C^2 = \left(\frac{3 v_C N_C P_{eq}}{4\pi}\right)^{2/3} \tag{23}$$

with $v_C$ as the volume of a repeat unit of the core polymer and $N_C$ as the degree of polymerization the following equation was derived:

$$P_{eq} = \left(\frac{6\gamma}{5 k_B T n N_{Sh} l^{5/3}}\right)^{18/11} 36\pi (N_C v_C)^2 \tag{24}$$

On the basis of this equation, $P_{eq}$ of the PEP−PEO/water system was calculated. Thereby, $l_b^2$ was taken as 2.1436 Å$^2$ and $C_\infty$ as 5.7, as measured by SANS for PEO homopolymers in the melt state.[34] The value of the surface tension between PEP and water is not known but is well approximated by $\gamma = 51.24 \times 10^{-3}$ N m$^{-1}$, the value of decane and water.[23] The volume of a PEP repeat unit, $v_c = v_{PEP}$ was calculated to be 1.3579 $\times 10^{-22}$ cm$^3$, the degrees of polymerization of the blocks, $N_C = N_{PEP} = 67.2$ and $N_{Sh} = N_{PEO} = 135.7$, were determined from the molecular weights $M_n$ of the PEP and PEO blocks, respectively. Thus, an aggregation number of 740 was calculated. Although the experimental result is higher by a factor of 3−4, this simple model well represents the unusual high aggregation number of this block copolymer/solvent system. According to eq 24 the high value of $P_{eq}$ is mainly a consequence of the large surface tension between PEP and water.

In a different model the micellar free energy $F$ is described by Halperin[13] on the basis of a spherical core/shell interface. In this view a different expression for $F_{Sh}$ is derived, since the spherical geometry leads to a radial size distribution of the blobs:[36]

$$\xi(r) \simeq r P_{eq}^{-1/2} \tag{25}$$

with $r$ as the distance from the center of the micelle. Using again the $k_BT$ per blob ansatz, the contribution $F_{Sh}$ is of the following form:

$$F_{Sh} \simeq k_B T P_{eq}^{1/2} \ln(R_M/R_C) \tag{26}$$

In this model the contribution of the stretching of the core chains can be introduced by

$$F_C \simeq k_B T P_{eq}^{2/3} N_C^{-1/3} \tag{27}$$

Thereby, a uniform stretching of all core chains is assumed. An analytical expression for $P_{eq}$ by minimizing $F$ cannot be derived by eqs 20, 25, 26, and 27. In order to obtain a solution, we have determined $P_{eq}$ graphically. By inserting the experimental values for $R_M$ and $R_C$ and the others, as already used in the former

calculation, the equilibrium aggregation number was found to be 350, which disagrees strongly with the experimental value of 2430. In a further step the contribution due to $F_C$ was omitted. Minimization of $F$ with respect to $P_{eq}$ becomes possible in this case, leading to

$$P_{eq} \simeq \left( \frac{8\pi\gamma(3/(4\pi)N_C v_C)^{2/3}}{3k_B T \ln (R_M/R_C)} \right)^{6/5} \quad (28)$$

Applying this equation yields $P_{eq}$ as 1100. In comparison with the former result of $P_{eq} = 350$, it becomes obvious that the contribution of $F_C$ to the free energy of the micelle is overestimated by the assumption that all core chains have to be stretched uniformly. Apparently, only a few chains have to be stretched to fill the core to constant density. In comparison with the experimental result, $P_{eq}$ is still smaller by a factor of ~2 but, however, both values show the same order of magnitude. Since the calculation was made on the basis of scaling laws, where an uncertainty is given by the proportionality used in the $k_BT$ per blob ansatz, the experimental and theoretical value can be regarded to be in good agreement.

In order to explain the high aggregation number, a comparison is made with the thoroughly investigated polystyrene-*block*-polyisoprene (PS−PI)/*n*-heptane or *n*-decane system. The main difference is that the surface tension, $\gamma = 5.92$ dyn/cm,[14] of PS and *n*-heptane is considerably smaller than the value, $\gamma = 51.24$ dyn/cm, estimated for PEP and water. According to eq 28, this difference leads to a ratio of 13.3 of the aggregation numbers, presuming that the other parameters are identical. A comparison on an experimental basis cannot be made directly since a PS−PI block copolymer having $N_C = 67.2$ and $N_{Sh} = 135$ repeat units has not been investigated. However, by using the semiempirical scaling relation $P_{eq} \sim N_C^2 N_{Sh}^{-18/11}$ given in ref 16, an aggregation number of $P_{eq} = 161$ can be estimated. The ratio between the experimental and the semiempirical number is about 15, which is close to the theoretical value of 13.3. This good agreement obtained on simple considerations clearly indicates that the driving force to the high aggregation number in the PEP−PEO/water system is the high surface tension between PEP and water.

A further theory of micellization of AB diblock copolymers in selective solvents was developed by Nagarajan and Ganesh.[14] Six different contributions to the micellar free energy are considered in this model. The reference state for the energy calculations is a single block copolymer chain in infinite dilution. The free energy of the shell, $F_{Sh}$, and of the core, $F_C$, consists of two terms. The first term includes entropy contributions of the block copolymer that are involved when passing from the reference to the micellar state. The second term includes contributions due to chain deformation. The basis for these calculations are mean field approximations. The expression for the interfacial free energy, $F_{int}$, is equal to the one introduced in the former models (eq 20). In the Nagarajan and Ganesh theory, the entropy loss arising from the localization of the joints, linking the two polymer blocks together, at a small region of the core−shell interface is also considered. By comparison of experimental data from three different copolymer/solvent systems and numerical results from the theory, the following scaling relation was established:

$$P_{eq} = \frac{4\pi m_C(\gamma l_S^2/k_B T) + (4\pi/3)m_C^{1/2} + (4\pi/3)m_{Sh}^{1/2}(R_C/D)}{1 + m_C^{-1/3} + (m_C/m_{Sh})(D/R_C)^2} \quad (29)$$

In this equation $l_S$ denotes the characteristic length of a solvent molecule, which is calculated from its volume $l_S = v_S^{1/3}$, $m_{C,Sh}$ are the ratios of the volumes of the core or shell block and a solvent molecule: $m_{C,Sh} = v_{C,Sh}/v_S$. $D/R_C$ refers to a dimensionless shell thickness with $D$ as the thickness of the shell.

For a comparison with our results, we took the radii $R_M = 294$ Å and $R_C = 176$ Å, as obtained from the model fitting. With $l_S = 3.1$ Å, $m_C = 305.17$, $m_{Sh} = 294.67$, and $\gamma = 51.24$ dyn/cm eq 29 predicts an equilibrium aggregation number of $P_{eq} = 2977$. By the use of the hydrodynamic radius, $R_H = 339$ Å, an aggregation number $P_{eq} = 2373$ is calculated, indicating that the value sensitively depends on which measured quantity is considered. In any case, the experimental aggregation number is well represented by this theory. Whether this good agreement is fortuitous or whether the mean field ansatz carries through also for a large range of compositions will be assessed by studies of PEP−PEO block copolymer systems where the composition is varied by a factor of 10. These studies are in progress.

## 5. Summary and Conclusion

In this work we have presented a study of the aggregation behavior of a model PEP−PEO amphiphilic block copolymer in water. The results obtained by SANS, DLS, and viscometry can be summarized as follows:

(i) At room temperature and in the concentration range investigated, the PEP−PEO block copolymer forms equilibrium micelles of a single size with low polydispersity.

(ii) The micelles are spherical in shape and consist of a pure PEP core and a highly swollen PEO corona. The core−shell interface as well as the density cutoff at the periphery of the micelle are fairly sharp.

(iii) The large aggregation number and the resulting huge dimension of the micelle are explained by the large surface tension between water and PEP in terms of free energy calculations.

The thermodynamic equilibrium of the micelles and the well-defined structure are important with respect to a quantitative interpretation in the framework of existing micellar theories. Therefore, the results of this study will serve as a starting point for a systematic investigation of the micellization behavior of this model block copolymer.

**Acknowledgment.** This work was performed in the framework of the project "self-organization of polymers and polymeric glasses", which is financially supported by the Deutsche Forschungsgemeinschaft. M. Zähres (Universität Duisburg) is gratefully acknowledged for the NMR measurements, and M. Monkenbusch (Forschungszentrum Jülich) and L. J. Fetters (Exxon Research & Engineering Co., Annandale, NJ) for helpful discussions.

## References and Notes

(1) Xu, R.; Winnik, M. A.; Hallett, F. R.; Riess, G.; Croucher, M. D. *Macromolecules*, **1991**, *24*, 87.

(2) Wilhelm, M.; Zhao, C.-L.; Wang, Y.; Xu, R.; Winnik, M. A.; Mura, J.-L.; Riess, G.; Croucher, M. D. *Macromolecules*, **1991**, *24*, 1033.
(3) Xu, R.; Winnik, M. A.; Riess, G.; Chu, B.; Croucher, M. D. *Macromolecules*, **1992**, *25*, 644.
(4) Caldérara, F.; Hruska, Z.; Hurtrez, G.; Lerch, J.-P.; Nugay, T.; Riess, G. *Macromolecules*, **1994**, *27*, 1210.
(5) Jada, A.; Hurtrez, G.; Siffert, B.; Riess, G. *Macromol. Chem. Phys.*, **1996**, *197*, 3697.
(6) Hickl, P.; Ballauff, M.; Jada, A. *Macromolecules*, **1996**, *29*, 4006.
(7) Yu, K.; Eisenberg, A. *Macromolecules*, **1996**, *29*, 6359.
(8) Allgaier, J.; Willner, L.; Richter, D. German Patent Application, No. P 19634477.8, 1996.
(9) Allgaier, J.; Poppe, A.; Willner, L.; Richter, D. *Macromolecules*, **1997**, *30*, 1582.
(10) Hillmyer, M. A.; Bates, F. S. *Macromolecules*, **1996**, *29*, 6994.
(11) Hillmyer, M. A.; Bates, F. S.; Almdal, K.; Mortensen, K.; Ryan, A. J.; Fairclough, J. P. A. *Science*, **1996**, *271*, 976.
(12) Halperin, A.; Tirrell, M.; Lodge, T. P. *Adv. Polym. Sci.*, **1992**, *100*, 31.
(13) Halperin, A. *Macromolecules*, **1989**, *22*, 3806.
(14) Nagarajan, R.; Ganesh, K. *J. Chem. Phys.*, **1989**, *90*, 5843.
(15) Ionescu, I.; Picot, C.; Duplessix, R.; Duval, M.; Benoit, H.; Lingelser, J. P.; Gallot, Y. *J. Polym. Sci.*, **1981**, *19*, 1033.
(16) Iatrou, H.; Willner, L.; Hadjichristidis, N.; Halperin, A.; Richter, D. *Macromolecules*, **1996**, *29*, 581.
(17) Richter, D.; Schneiders, D.; Monkenbusch, M.; Willner, L.; Fetters, L. J.; Huang, J. S.; Lin, M.; Mortensen, K.; Farago, B. *Macromolecules*, **1997**, *30*, 1053.
(18) Yamaoka, H.; Matsuoka, H.; Sumaru, K.; Hanada, S.; Imai, M.; Wignall, G. *Physica B*, **1995**, *213 & 214*, 700.
(19) Marx-Figini, M.; Figini, R. V. *Makromol. Chem.*, **1980**, *181*, 2401.
(20) Russel, T. P.; Lin, J. S.; Spooner, S.; Wignall, G. D. *J. Appl. Crystallogr.*, **1988**, *21*, 629.
(21) Brown, W. *Dynamic Light Scattering*; Oxford University Press: Oxford, U.K., 1993.
(22) Pecora, R.; Berne, B. J. *Dynamic Light Scattering*; J. Wiley & Sons: New York, 1976.
(23) Landolt; Börnstein. In *Zahlenwerte und Funktionen*; Bartels, J., Tenbruggencate, P., Hellwege, K. H., Schäfer, K., Schmidt, E., Eds.; Berlin-Göttingen-Heidelberg, 1956.
(24) Koppel, D. E. *J. Chem. Phys.* **1972**, *57*, 4814.
(25) Provencher, S. W. *Comput. Phys. Commun.* **1982**, *27*, 229.
(26) Provencher, S. W. *Comput. Phys. Commun.* **1982**, *27*, 213.
(27) Pedersen, J. S.; Posselt, D.; Mortensen, K. *J. Appl. Crystallogr.* **1990**, *23*, 321.
(28) Vennemann, N.; Lechner, M. D.; Oberthür, R. C. *Polymer*, **1987**, *28*, 1738.
(29) Selser, J. C. *Macromolecules*, **1979**, *12*, 909.
(30) Devanand, K.; Selser, J. C. *Nature*, **1990**, *343*, 739.
(31) Štěpánek, P. *J. Chem. Phys.* **1993**, *99*, 6384.
(32) Brown, W. *Polymer*, **1985**, *26*, 1647.
(33) Porsch, B.; Sundelöf, L.-O. *Macromolecules*, **1995**, *28*, 7165.
(34) Smith, G. D.; Yoon, D. Y.; Jaffe, R. L.; Colby, R. H.; Krishnamoorti, R.; Fetters, L. J. *Macromolecules*, **1996**, *29*, 3462.
(35) Alexander, S. *J. Phys. (Paris)*, **1977**, *38*, 977.
(36) Daoud, M.; Cotton, J. P. *J. Phys.* **1982**, *43*, 531.

MA970470M